MONTE CARLO ASSESSMENT OF SAMPLING UNCERTAINTY OF CLIMATE CHANGE IMPACTS ON WATER RESOURCES YIELD IN YORKSHIRE, ENGLAND

N. R. NAWAZ[1] and A. J. ADELOYE[2]

[1]*Lecturer, Dept. Geography, University of Leeds, LS2 9JT, United Kingdom*
E-mail: N.R.Nawaz@leeds.ac.uk
[2]*Senior Lecturer, School of the Built Environment, Heriot-Watt University, Edinburgh, EH14 4AS, United Kingdom*
E-mail: A.J.Adeloye@hw.ac.uk

Abstract. Despite much effort over the last decade, there still remain many uncertainties in the assessed impacts of climate change on water resources. This study has carried out Monte Carlo Simulations to characterise the sampling uncertainties in assessed water resources impacts. The investigation employed data from catchments in northeast England, which incorporate water supply reservoirs. The impacts assessment used scenarios from three GCM experiments: (i) the Canadian first generation coupled model (CGCM1), (ii) the Australian first generation coupled model (CSIRO-mk2b) and (iii) the British third generation model (HadCM3). The results showed that yield impacts are subject to wide variability, irrespective of the GCM experiment, which calls for caution when using mean impacts obtained from single data record analysis for decision making.

1. Introduction

Many studies have been carried out in recent times to assess the impact of climate change on water resource systems (see www.pacinst.org/topics/global_change/water_bibliography/ for a comprehensive bibliography). Water resources impact assessment often involves three distinct stages. The first stage is to construct catchment-scale General Circulation Model (GCM) based climate change scenarios and use these to perturb baseline (current) climate to obtain future climate. This is then followed by forcing a catchment response model with both the current and future climate to obtain the corresponding runoff records. Finally, the hydrological data series are then input into a water resource simulation model to obtain possible impacts. Because of the uncertainties introduced at successive stages of the assessment, it is important that the assessed impacts are viewed with caution (Hulme et al., 1999).

1.1. UNCERTAINTIES IN CLIMATE IMPACTS ASSESSMENT

Three major sources of uncertainty have been cited by Carter et al. (1999) and these arise as a result of:

Climatic Change (2006) 78: 257–292
DOI: 10.1007/s10584-005-9043-9

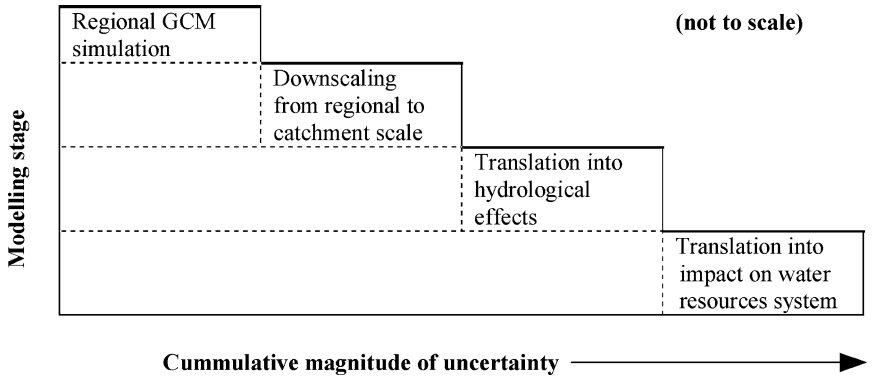

Figure 1. Schematic of the levels of uncertainty in successive stages of climate impact assessment (note the incremental uncertainties are not necessarily equal).

1. Difficulty in predicting future levels of greenhouse gas (GHG) and aerosol emissions;
2. Differences in global climate of sensitivity of different GCMs. This is due to differences in the way physical processes and feedbacks are simulated in different models;
3. Uncertainties in regional climate change apparent from differences in regional estimates of climate change by different GCMs, for the same mean global warming.

When climate change scenarios are used to assess the implications for water resource systems, then further sources of uncertainty are introduced. These comprise data and modelling uncertainties (Prudhomme et al., 2003, Wood et al., 1997). Uncertainties in hydrologic data arise due to inaccurate measurements and the sampling procedure. A relatively short rainfall or runoff record (e.g. 30 years of daily data) rarely incorporates the complete range of possible extremes, and wet and dry period lengths. Re-sampling techniques will allow evaluation of this uncertainty (Prudhomme et al., 2003). Model uncertainties arise because of the imprecision in hydrological and water resource systems modelling. Both the model structure and the parameters are uncertain. Indeed, the commonly adopted assumption that model parameters remain valid in a future changed climate is not valid. The range of uncertainties are summarised in Figure 1.

1.2. QUANTIFYING UNCERTAINTIES IN CLIMATE IMPACTS ASSESSMENT: SOME STUDIES TO DATE

Some studies have attempted to quantify some of the uncertainties (discussed in section 1.1) including Prudhomme et al. (2003), Shackley et al. (1998), Nikolaidas et al.

(1994), Mimikou et al. (2000), Cameron et al. (2000a), and Sankarasubramanian et al. (2001).

Prudhomme et al. (2003) randomly generated 25,000 climate scenarios for the UK by adopting a Monte Carlo simulation based on several GCMs and different greenhouse gas emissions scenarios. Future flood scenarios were compared to current conditions. Most scenarios showed an increase in both the magnitude and the frequency of flood events, generally not greater than the 95% confidence limits. The largest uncertainty was attributed to the type of GCM used, with the magnitude of changes varying by up to a factor of 9 in Northern England and Scotland. On this basis, Prudhomme et al. (2003) concluded it is essential that climate change impact studies consider a range of climate scenarios derived from different GCMs,

Shackely et al. (1998) used a global carbon cycle model and historical carbon dioxide emissions levels to generate a large number of possible future carbon dioxide scenarios. Their output showed a greater variability in future carbon dioxide levels than those obtained using deterministic models. Although Shackley et al. (1998) did not subsequently use the stochastically generated emissions scenarios to force a climate model to obtain a large number of climate scenarios, such is entirely feasible with the aid of a simple climate model.

The study of Nikolaidas et al. (1994), on the other hand, concentrated on the sampling uncertainty. They used eight years of daily historical meteorological data from a catchment in Vermont, USA to stochastically generate 50 sequences of precipitation, air temperature, dew point, wind speed, solar radiation, and cloud cover. They then used these data in conjunction with a modified Enhanced trickle-Down (ETD) conceptual hydrological model (Nikolaidas et al., 1993) to determine the effects on runoff. They showed the range of input uncertainty in baseline mean annual runoff to be $\pm 24.2\%$. These results were then compared with those obtained from deterministic modelling and climate change scenarios based on the Geophysical Fluid Dynamics Laboratory (GFDL) and the Goddard Institute for Space Studies (GISS) GCMs. The GFDL and GISS predicted reductions in annual runoff of 37.5% and 17.9%, respectively. The two GCMs impacts were both predicting reductions in runoff. However, when the sampling uncertainty in the inputs was incorporated by Nikolaidas et al. (1994) the results showed that the runoff could actually increase by 24%. Since the statistical description of the impacts is a natural end-product of the Monte Carlo simulation experiments, the probability of actually having the 24% increase in runoff can be estimated.

Quantification of sampling uncertainty was also the subject of a study by Mimikou et al. (2000). They investigated a catchment in central Greece and used one scenario from the HadCM2 transient experiment and another from the UKHI equilibrium experiment - both representative of the 2040–69 period. The impact assessment proceeded in two stages. The first stage involved using baseline historical data (1960–1996) to generate 50 sequences of precipitation and temperature data using respectively the lag-one and lag-two stochastic autoregressive models (AR(1)

and AR(2)). The second stage involved applying the climate change scenarios to the generated time-series data to obtain 50 sequences of future (1996–2050) precipitation and temperature. Both the baseline and future sequences were then fed in to the rainfall-runoff model to obtain the impacts on mean monthly runoff. Results showed that future mean monthly runoff resulting from the HadCM2 scenario was less than baseline runoff in all months of the year. The pattern of change was for largest runoff reductions during the summer (especially in June and August when up to a 46% reduction was expected). The expected winter reductions (of about 13%) were more moderate, especially during January, March and December while the change in mean annual runoff was −18.4%.

Cameron et al. (2000b) explored the effects of hydrologic model parameter uncertainties on flood frequency for a small Welsh catchment in the UK. They used 1000 rainfall and streamflow model parameter sets to generate separate 1000 year continuous hourly rainfall and streamflow time series data. To study the effects of climate change, UKCIP98 scenarios were employed (now superseded by UKCIP02 scenarios) which were developed by the UK Climate Impacts Programme (UKCIP) using output from HadCM2. The UKCIP98 scenarios were designed to add "detail" to the coarse-resolution HadCM2 scenarios ($2.5^\circ \times 3.75^\circ$) by the so-called "unintelligent" downscaling. The term *unintelligent* is used since the downscaling method, simple linear interpolation, adds no useful information to the coarse-scale scenario. UKCIP98 scenarios are available at a spatial resolution of 10 km × 10 km. The scenarios were used to investigate the impacts of climate change on the hourly annual maximum flood peaks of both short and long return periods (e.g. 10–100 years). Cameron et al. (2000b) reported that the risk of a given streamflow being realised changed under a different climate. Moreover, the flood risk was significantly sensitive to model parameters. Four parameters were varied in the sensitivity study (these were selected on the basis that they are the most important in the control of the hydrologic model's simulated catchment response): (i) an exponential scaling parameter, (ii) effective available water capacity of the root zone, (iii) mean log transmissivity of the soil at saturation of the surface, and (iv) standard deviation of log transmissivity. Cameron et al. (2000b) concluded that there is a need to account explicitly for uncertainty within hydrological modelling, especially in estimating the impacts of climate change.

More recently, Sankarasubramanian et al. (2001) adopted a Monte Carlo simulation approach to investigate the influence of hydrologic model parameters on runoff. They investigated catchments in California, Colorado and Arkansas and adopted the concept of elasticity (i.e. proportional change in runoff divided by the proportional change in a climatic variable such as precipitation) for quantification of the sensitivity of streamflow to changes in climate. They used a Monte Carlo simulation technique to generate 10,000, 50-year sequences of annual precipitation and potential evapotranspiration. These sequences were then fed into three different annual rainfall-runoff models of increasing complexity to synthesise the corresponding runoff sequences. These are:

(i) Simple linear statistical model in which streamflow is related to precipitation (P) and potential evapotranspiration (PE);
(ii) Three-parameter nonlinear hydrologic model. This model relates P to evapotranspiration, groundwater storage, groundwater outflow and streamflow using only P as a model input.
(iii) Four-parameter nonlinear hydrologic model which accepts both P and PE as input, to simulate streamflow. Model capability also includes simulation internally of soil moisture store, groundwater store & outflow, and actual evapotranspiration.

Further model details are provided in Sankarasubramanian et al. (2001).

They then used a nonparametric approach along with the generated precipitation and runoff data to evaluate the precipitation elasticity of streamflow. Use of 10,000 data sequences allowed evaluation of the bias and root-mean-square error associated with the elasticity. The main conclusion reached was that in addition to being influenced by climate, streamflow is also sensitive to model parameters.

Although the aforementioned studies incorporated uncertainty analysis in climate change water resources impacts assessments, the assessed impacts have been limited to the runoff. In addition, many previous studies have investigated the stochasticity of climate change runoff impacts (e.g. Mimikou et al. (2000); Nikolaidas et al. (1994)) and for extremely simplified water resources systems, there are readily usable reservoir yield models for translating mean annual runoff uncertainties to yield uncertainties (see McMahon and Adeloye, 2005). However, for real, complex water resources systems such as the one analysed in the study, there are countless other factors – reservoir storage size, configuration of reservoir systems, the reliability and other performance attributes of the system, the system operating policy etc. – which are as important as the runoff. It is therefore not realistic to infer yield uncertainties from the runoff uncertainties alone for such systems. This was why this study has directly investigated the uncertainties of yield impacts as caused by predicted climate change.

Where a water resources system incorporates reservoirs, examining the runoff alone does not give the complete picture of how the system will behave under a changed climate. Instead, the storage-yield-performance relationship which integrates the effect of the runoff, demand and system operational strategies is a more appropriate characteristic to use (Nawaz and Adeloye, 1999). Thus, in the present study, the storage-yield-performance characteristics of a water supply reservoir in northeast England will also be examined.

2. Methodology

The impact assessment methodology, based on recommended protocol (Carter et al., 1994; 1999), is summarised in Figure 2.

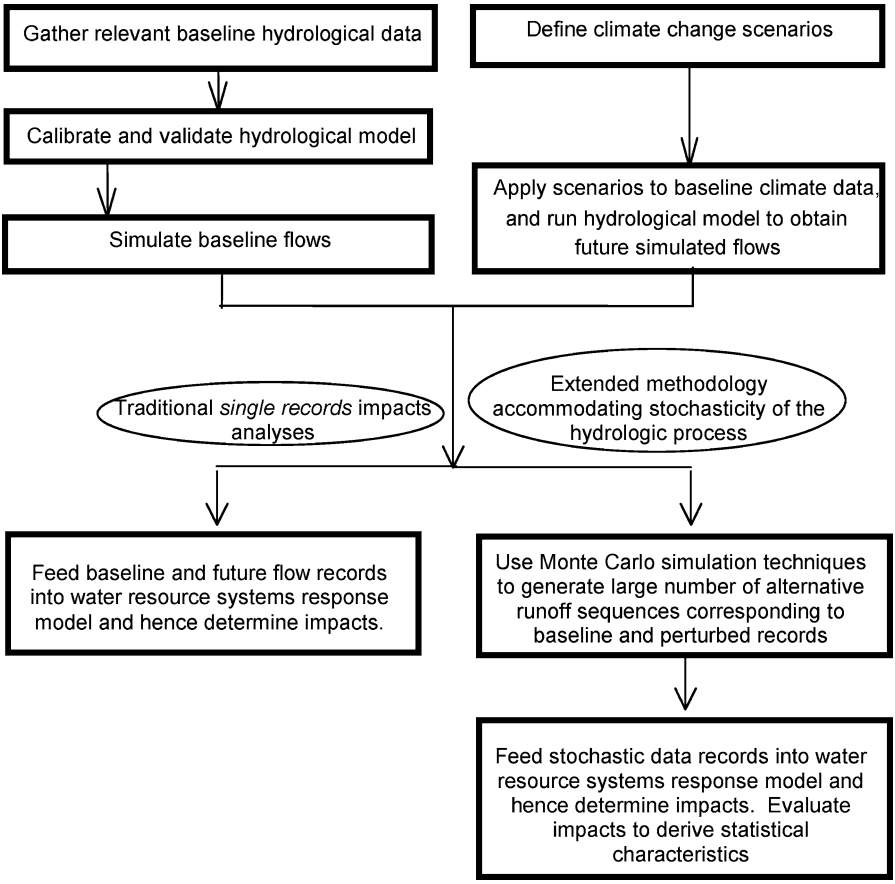

Figure 2. Deterministic and stochastic methodologies for climate change water resources impacts assessment (note the stochastic methodology enables sampling uncertainty of the impacts to be characterised).

Several sources of uncertainty in climate impacts assessment were identified in Section 1.1. This study is limited to quantifying only the sampling uncertainty which arises due to relatively short periods of hydroclimatological data records.

2.1. HYDROLOGIC MODELLING

The hydrologic modelling used the daily water balance model MODHYDROLOG (Chiew and McMahon, 1994). MODHYDROLOG is a conceptual daily rainfall-runoff model structured around five moisture stores as shown in Figure 3. All five stores are inter-related by catchment processes shown in Figure 3.

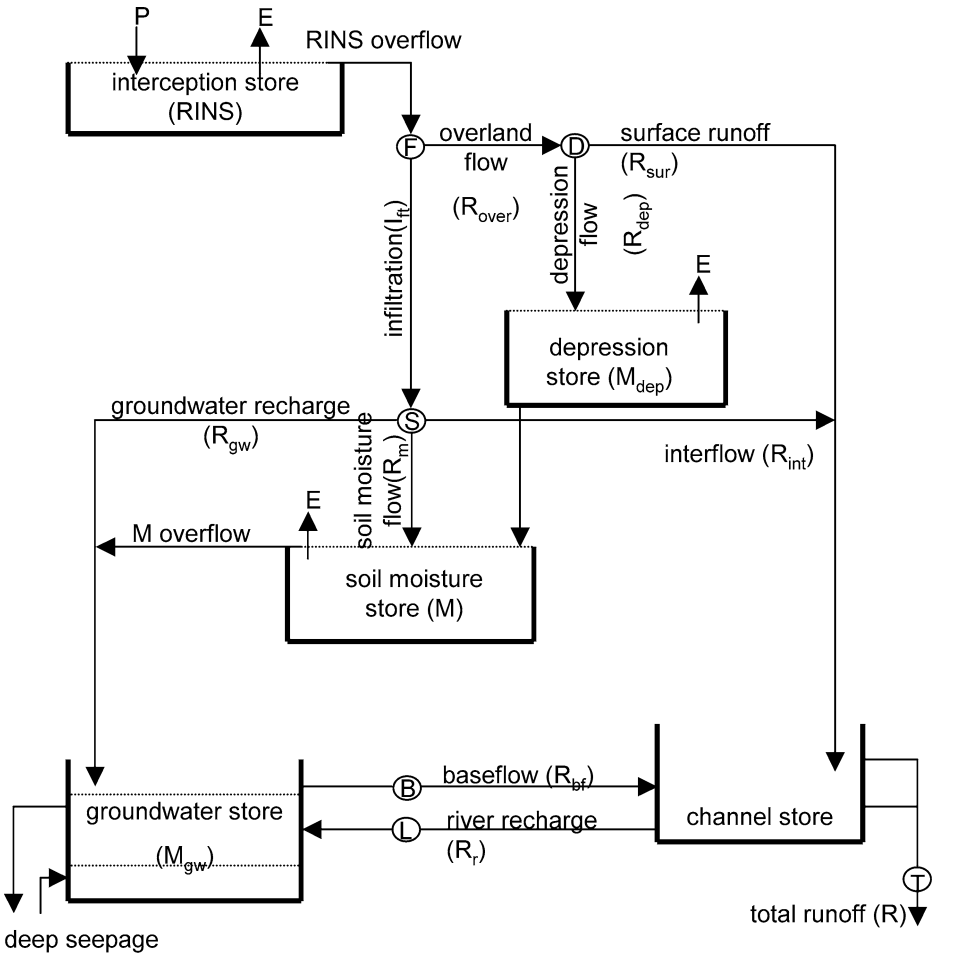

F = Infiltration function
D = Depression flow function
S = Soil moisture function
B = Baseflow function
L = River recharge function
T = Nonlinear routing function (with parameters a_{co} and a_{power} for storage delay)

Figure 3. Schematic of MODHYDROLOG (adapted from Chiew and McMahon, 1994, with modifications).

A summary of these processes (adopted from Pitman and Chiew, 1996) is provided. MODHYDROLOG conceptualizes the catchment as five inter-connected stores (i) interception store, (ii) depression store, (iii) soil moisture store, (iv) groundwater store, and (v) channel store. In MODHYDROLOG, daily rainfall first fills the interception store which is emptied daily by evaporation. The excess rainfall is then subjected to a function which determines infiltration. The water that does not infiltrate is diverted to a depression store (controlled by the depression flow function) and the remaining water becomes surface runoff. The emptying of the depression store takes place via both evapotranspiration and delayed infiltration into the soil moisture store. A soil moisture function is then applied to all infiltrated soil moisture. This function diverts moisture to the streamflow in the form of interflow and to the groundwater store as groundwater recharge. Un-diverted moisture enters the soil moisture store. Evapotranspiration from the soil moisture store takes place at a rate that depends on soil moisture status up to a maximum equal to the potential evapotranspiration. The soil moisture store has a finite capacity and overflows into the groundwater store. The groundwater store can be reduced by baseflow into the stream and also by deep seepage to the underlying aquifers, or recharged by the stream and vertical (upwards) movement from the underlying aquifers.

A detailed description of MODHYDROLOG is provided by Chiew and McMahon (1994). The model requires daily precipitation and potential evapotranspiration as input and simulates groundwater recharge in addition to runoff. The model, which has 19 parameters (see Chiew and McMahon, 1994; Reungoat, 2000 for details), simulates soil moisture and surface water movement and has been extensively tested in arid and temperate climates and used in a number of climate impacts investigations. However, in an application of the model to test catchments in Yorkshire, England, Reungoat (2000) found that the model is mostly sensitive to only seven of these parameters, implying that not all the 19 parameters need be optimised when calibrating the model. As expected, the influential parameters requiring optimisation (or calibration) are those describing the important processes such as canopy interception, infiltration, actual evapotranspiration, interflow and soil moisture storage capacity. Reungoat (2000) suggested that nothing would be lost by setting the non-optimised parameters to their default values based on knowledge of the characteristics of the catchment under investigation.

2.2. RESERVOIR PLANNING ANALYSIS

Reservoir planning analysis was achieved using the modified sequent peak algorithm (SPA) (Adeloye et al., 2001) which is an extension of the basic SPA (Thomas and Burden, 1963). The basic SPA estimates the failure-free capacity of an initially full single reservoir as the maximum of all the sequential deficits obtained using

(Loucks et al., 1981):

$$K_{t+1} = \begin{cases} K_t + D_t + \widehat{E}_t - Q_t; & \text{if} > 0.0 \\ 0.0; & \text{otherwise} \end{cases};$$
$$t = 1, 2, \ldots, T,\ T+1,\ T+2, \ldots, 2T \quad (1)$$

where K_t and K_{t+1} are the volumetric sequential deficits at the beginning and end of period t respectively; Q_t is the volumetric inflow during t; D_t is the volumetric demand during t; $\widehat{E}_t$ is the volumetric reservoir surface net evaporation (i.e. direct evaporation less direct rainfall) during t; and T is the total number of periods. Because $\widehat{E}_t$ depends on the exposed surface area of the reservoir, which in turn depends on storage, it cannot be explicitly included in the basic SPA. Therefore, a modified version of the basic SPA was used which is able to incorporate reservoir net surface evaporation, and also, reservoir performance metrics (see Lele (1987), Adeloye and Montaseri (1998), and Adeloye et al. (2001) for further details). A further benefit of the modified SPA lies in its ability to impose a limit on supply shortfall during failure periods which means that system's vulnerability or volumetric failure risk (Hashimoto et al., 1982) can be selected *a priori*. The recent modification carried out by Adeloye et al. (2001) allowed the SPA to be applicable to multiple reservoir systems.

Given that the SPA is primarily a reservoir capacity estimation tool, estimation of reservoir yield for a fixed storage capacity first requires derivation of the complete storage-yield function. Once determined, it is then a simple matter to determine the yields corresponding to any given capacity. This was the way the modified SPA was used in the study.

2.3. MONTE CARLO EXPERIMENTS

The generation of alternative runoff data utilised a parametric, multivariate annual lag-one autoregressive (AR(1)) model. This enabled generation of streamflow simultaneously at a number of sites, taking into account the covariances of the runoff. This is important for the multi-reservoir system configurations analysed in the study. In a study of climate change, it is also important that the stochastic modelling accounted for any covariances between the baseline and future runoff series. To achieve this, the baseline and future runoff series were considered as a bivariate pair, modelled as a fictituous two-site problem with the baseline representing one site and the future at this site being the second site. Thus for example for 3 site problem, the stochastic modelling will be formulated as a fictituous 6-site problem, i.e. all the three baseline runoff being the first 3 sites and the 3 future series representing the remaining 3 sites.

Once the annual flows had been generated, these were disaggregated to monthly flows using a Valencia-Schaake (VS) (Valencia and Schaake, 1973) dissagregation scheme. The coupled multivariate annual AR(1)-VS model was used to generate 1000 replicates of monthly baseline-future runoff pairs having the same length as the assumed baseline or future record.

An important step in generating stochastic streamflow was the selection of an appropriate distribution for the streamflow data. Of the various techniques available, the probability plot correlation coefficient (PPCC) test was employed. It was decided to test the monthly and annual streamflow data for five distributions using the PPCC test (Filliben, 1975). The five distributions considered were the normal, two-parameter log-normal (LN2), the three-parameter log-normal (LN3), Gamma and the log Pearson type 3 (LP3) distributions. In the PPCC test, the correlation coefficient between an observed series and the corresponding series produced by fitting an assumed distribution to the data is calculated. The closer this correlation coefficient to unity, the greater the evidence of the appropriateness of the fitted distribution.

In the case of annual flow, the selection of the most appropriate distribution was straightforward since the test output comprised five correlation coefficients corresponding to the five distributions tested. The most appropriate distribution was the one which provided the highest correlation coefficient. As far as the monthly flows were concerned, selecting the most appropriate distribution was less straightforward. This is because different distributions are appropriate in each particular month. Ideally, therefore, the best distribution should be selected for each month. Clearly, such an approach would be rather tedious. An alternative approach was adopted in which a score was assigned to a particular distribution by summing the total number of occasions it yielded the highest correlation coefficient. The distribution which resulted in the highest score would then be used in modelling all the twelve months of the year. The analysis revealed that the annual and monthly flows are best represented by a normal and LP3 distributions, respectively.

After determining appropriate probability distributions for generating streamflow, the performance of the stochastic model was assessed. A comparison of selected statistical parameters (e.g. mean flow, CV etc.) indicated that the model was preserving all the statistics of the historical data record adequately. Performance of the streamflow generator is summarised later (section 4.2).

3. Case Study

3.1. CATCHMENT AND DATA

The reservoirs are located in Yorkshire, northeast England and consist of three direct catchments namely Hebden, Luddenden, and Ogden. Hebden (which comprises three sub-catchments; Gorple, Widdop and Walshaw Dean) is the largest of

the catchments with a total area of 26.43 km^2. Luddenden is much smaller with an area of 6.46 km^2 and Ogden is the smallest of the three (5.39 km^2). These catchments are located between 53° 41′ and 53° 50′ northern latitude, and 1° 53′ and 2° 10′ western longitude as shown in Figure 4. The catchments are situated at relatively moderate altitudes; ranging from 370 m (Luddenden) to 400 m (Ogden) above sea level. Land cover is mainly grass with some trees, and the surface soil mainly consists of hill peat. The climate in the region can be described as temperate with mean (1961–1990) annual temperature of about 8.2°C and the average annual precipitation recorded as 1425 mm at Hebden, 1113 mm (Luddenden) and 1081 mm (Ogden). Corresponding mean annual runoff is 1000 mm (Hebden), 825 mm (Luddenden) and 829 mm (Ogden).

The system comprises a total of eleven inter-linked reservoirs and is therefore a fairly complex system as shown in Figure 5. If, however, the reservoirs in parallel are grouped, then the system simplifies to a five-reservoir system (Gorple, Widdop, Walshaw Dean, Luddenden, and Ogden). The reservoirs provide water for domestic and industrial purposes, as well as compensation releases, and they are operated to satisfy the full demand at all times, although during extreme droughts, reductions in releases can be made.

3.2. HYDROCLIMATOLOGICAL DATA

Daily baseline (1961–1990) data of precipitation and runoff were made available by Yorkshire Water Services Ltd (YWS). Precipitation data were available at five gauge stations, namely Gorple, Widdop, Walshaw Dean, Luddenden and Ogden (see Figure 5).

Runoff data were also provided by YWS for the three Hebden sub-catchments; Gorple, Walshaw Dean, and the remaining two catchments; Luddenden and Ogden. Additionally, minimum and maximum daily temperature, and observed daily number of sunshine hours were provided by the British Atmospheric Data Centre (BADC). These data were also available for the baseline (1961–1990) period.

The daily data were aggregated to monthly data with which to calculate the monthly averages. Mean annual precipitation and runoff for the catchments are given in Table I. Monthly and annual data on climatological variables such as sunshine hours and temperature are provided in Table II. Daily PE data were available at Gorple site within Hebden catchment (see Figure 4) and the average annual and monthly values are also given in Table II. These data were derived by Mott MacDonald (1995) using the Penman equation (Penman, 1950; MAFF, 1967). In the absence of PE data at the other sites, it was assumed that PE at all sites is equivalent to Gorple PE. Although this assumption may not be strictly valid, given that the catchments are located in a temperate region, and in close proximity to each other, then any small differences in PE at the different sites should not have any major impact on the climate impacts assessment. As seen in Tables I and II, on an

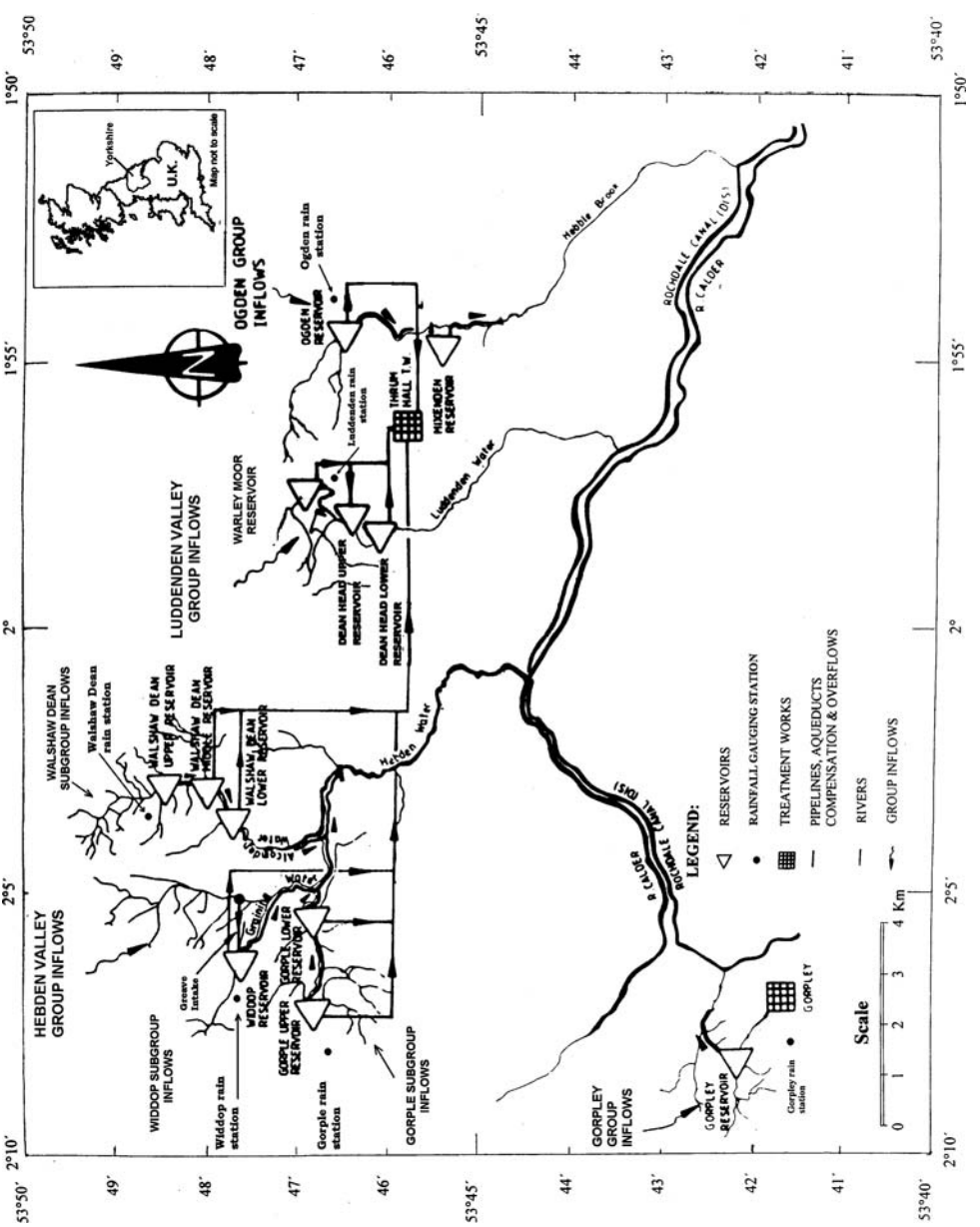

Figure 4. Detailed map of the catchment (adopted from Yorkshire Water RRDY, 1991, with modifications).

TABLE I
Characteristics of the catchments analysed

Catchment	Area (km^2)	Mean annual runoff (mm)	Mean annual rainfall (mm)
Gorple	8.02	989.4	1469.9
Widdop	9.00	1025.1	1413.4
W. Dean	9.41	985.4	1397.1
Luddenden	6.46	824.5	1112.9
Ogden	5.39	828.9	1081.4
Group total	38.28	946.3	1323.8

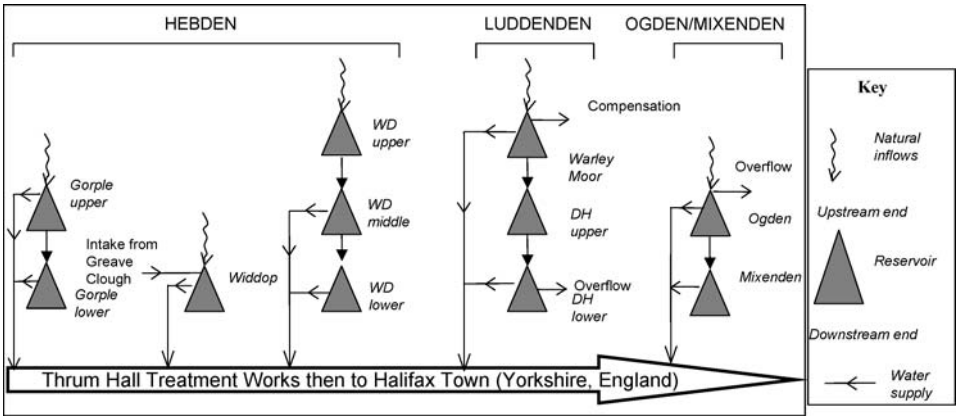

Figure 5. Schematic configuration of the reservoir systems.

annual basis, the rainfall far exceeds the potential evapotranspiration, implying that significant soil moisture deficits rarely develop in these catchments.

Open-water evaporation would be required in reservoir analysis to take account of reservoir surface fluxes. Empirical data were unavailable and the PE was converted to open-water (E_0) evaporation using the formulation of Penman (1950); $E_0 = PE/f$, where f is dependent on the season. For (i) summer (May, June, July, August), $f = 0.8$, (ii) winter (November, December, January, February), $f = 0.6$ and, (iii) equinoctial months (March, April, September, October), $f = 0.7$ (Shaw, 1994). The calculated mean monthly open-water evaporation rate is given in Table II.

3.3. CLIMATE CHANGE SCENARIOS

There are a number of GCMs available for use in climate impacts assessments; the selection of appropriate models will be dictated by the ease of GCM data access and whether the required climatological variables are available. GCM selection

TABLE II
Mean monthly historical climatological data for west Yorkshire (1961–1990)

Month	Observed number of sunshine hours (n)	Maximum theoretical number of sunshine hours (N)	Total short-wave radiation received at top of atmosphere, R_a (w/m^2)	Min. temp. (°C)	Max. temp. (°C)	Ave. temp. (°C)	PE[a] (mm)	E_0[b] (mm)
Jan	35.0	246.3	51.2	0.4	5.0	2.7	12.9	21.5
Feb	53.4	272.2	108.2	0.3	4.9	2.6	15.5	25.8
Mar	90.1	363.0	224.5	1.6	7.1	4.3	33.4	47.7
Apr	123.2	416.7	338.3	3.2	9.8	6.5	50	71.4
May	164.3	491.9	455.7	6.1	13.7	9.9	79.5	99.4
Jun	162.6	505.7	492.7	9.2	16.7	12.9	82.4	103.0
Jul	156.0	510.1	485.3	11.0	18.2	14.6	84.2	105.3
Aug	146.0	458.1	394.4	10.8	17.8	14.3	74.1	92.6
Sep	114.4	381.0	261.3	9.0	15.5	12.3	52	74.3
Oct	80.8	325.8	153.9	6.6	12.2	9.4	31.1	44.4
Nov	53.0	256.0	67.9	2.9	7.8	5.4	17.5	29.2
Dec	28.2	230.8	35.4	1.3	5.9	3.6	12.4	20.7
Annual	1206.9[c]	3068.7[c]	255.7	5.2	11.2	8.2	545.0	735.3

[a]Potential evapotranspiration based on daily time-series data at Gorple site (supplied by Yorks. Water).
[b]Open water evaporation based on daily time-series data at Gorple site (calculated by factoring PE).
[c]Annual accumulation.

therefore requires a consideration of the following (Smith and Hulme, 1998):

(i) whether to restrict choice only to the latest models;
(ii) GCM spatial resolution;
(iii) GCM performance in simulating observed climate;
(iv) representativeness of results, e.g. a selection of three GCMs, giving, average, low and high-end range of all GCM experiments.

Indeed, Carter et al. (1999) emphasised using more than one GCM in impacts assessments to investigate differences in model output. Based on these and other criteria, the IPCC recommended seven GCMs for impact assessments. For this investigation it was decided to apply the results from three of these:

(i) CGCM1 – Canadian Centre for Climate Modelling and Analysis GCM no. 1 (Boer et al., 2000);
(ii) CSIRO1 (also known as CSIRO-mk2b)- Australian Commonwealth Scientific and Industrial Research Organisation, first generation atmosphere-ocean coupled GCM (Hirst et al., 2000);
(iii) HadCM3 – UK Hadley Centre for Climate Prediction and Research Coupled Model no. 3 (Gordon et al., 2000).

The CGCM1 simulation experiment is based on observed carbon dioxide and sulphate aerosol forcing from 1850 to 1989 and a 1% per year compound increase from 1990–2100 based on the IS92a emissions scenario. The effects of instantaneous carbon dioxide doubling (plus sulphate aerosol effects) lead to a 3.5°C global mean surface air temperature rise - known as the equilibrium climate sensitivity.

The CSIRO1 simulation experiment is based on observed carbon dioxide forcing (sulphate aerosol forcing is excluded) from 1880 to 1989 and a 0.9% per year compound increase from 1990–2100 based on the IS92a emissions scenario. The effects of carbon dioxide doubling without sulphate aerosol effects gives an equilibrium climate sensitivity of 4.3°C.

The HadCM3 simulation experiment is based on observed carbon dioxide forcing (sulphate aerosol forcing is excluded) from 1860 to 1989 and a 1% per year compound increase from 1990–2100 based on the IS92a emissions scenario. The equilibrium climate model sensitivity is 3.3°C. The three GCM experiments are summarised in Table III. Further details of each of the three GCMs, CGCM1, CSIRO1 and HadCM3 can be found in Flato et al. (2000), Gordon and O'Farrel (1997), and Gordon et al. (2000), respectively.

Since GCM output is at a relatively coarse spatial scale, temperature, radiation and precipiation were downscaled to the catchment scale using linear interpolation which involved using the four GCM grid points nearest to the catchment (von Storch et al., 1993). The interpolation was carried out on the basis of linear averaging by the inverse of distance between the catchment and the four GCM grid points (see Smith et al., 1992). The advantage of this approach is that it allows regional climate change scenarios to be defined that would otherwise be difficult or costly to obtain. Besides,

TABLE III
Summary information on the CGCM1, CSIRO1 and HadCM3 experiments

Climate Modelling Centre	Canadian Climate Centre	Commonwealth Scientific & Industrial Research Organisation, Australia	Hadley Centre, UK
Model name	CGCM1	CSIRO1	HadCM3
Atmospheric horizontal resolution (latitude by longitude)	3.75° × 3.75°	3.2° × 5.6°	2.5° × 3.75°
Atmospheric vertical resolution (layers)	10	9	19
Oceanic horizontal resolution (latitude by longitude)	1.8° × 1.8°	3.2° × 5.6°	1.25° × 1.25°
Oceanic vertical resolution (layers)	29	21	20
Treatment of atmosphere-ocean coupling	Flux-adjusted	Flux-adjusted	Not flux-adjusted
Treatment of land-surface processes	Modified bucket for soil moisture	Soil layers, plant canopy, and leaf stomatal resistance included	Soil layers, freezing and thawing of soil layers, plant canopy, and leaf stomatal resistance included
Treatment of multiple greenhouse gases	No, CO_2 used as surrogate	No, CO_2 used as surrogate	Yes
Transient climate sensitivity °C	3.5	4.3	3.3
Transient CO_2 forcing	1% pa compound	0.9% pa compound	1% pa compound
Greenhouse gases forcing	Historic, 1850–1989 IS92a, 1990–2100	Historic, 1881–1989 IS92a, 1990–2100	Historic, 1860–1989 IS92a, 1990–2100
Sulphate aerosol forcing	Historic, 1860–1989 IS92a, 1990–2100	None	None

other more sophisticated downscaling schemes such as statistical downscaling have been shown to be characterised by huge uncertainties (Wilby and Wigley, 1997). It was felt that the use of the simple linear downscaling would remove the extra dimension of uncertainty. The simple linear interpolation formulation applied is defined as (Smith et al., 1992):

$$\mathrm{VAR}_D = \frac{\sum^{i} \left(\frac{1}{D_i^s}\right) \mathrm{VAR}_i}{\sum \left(\frac{1}{D_i^s}\right)} \tag{2}$$

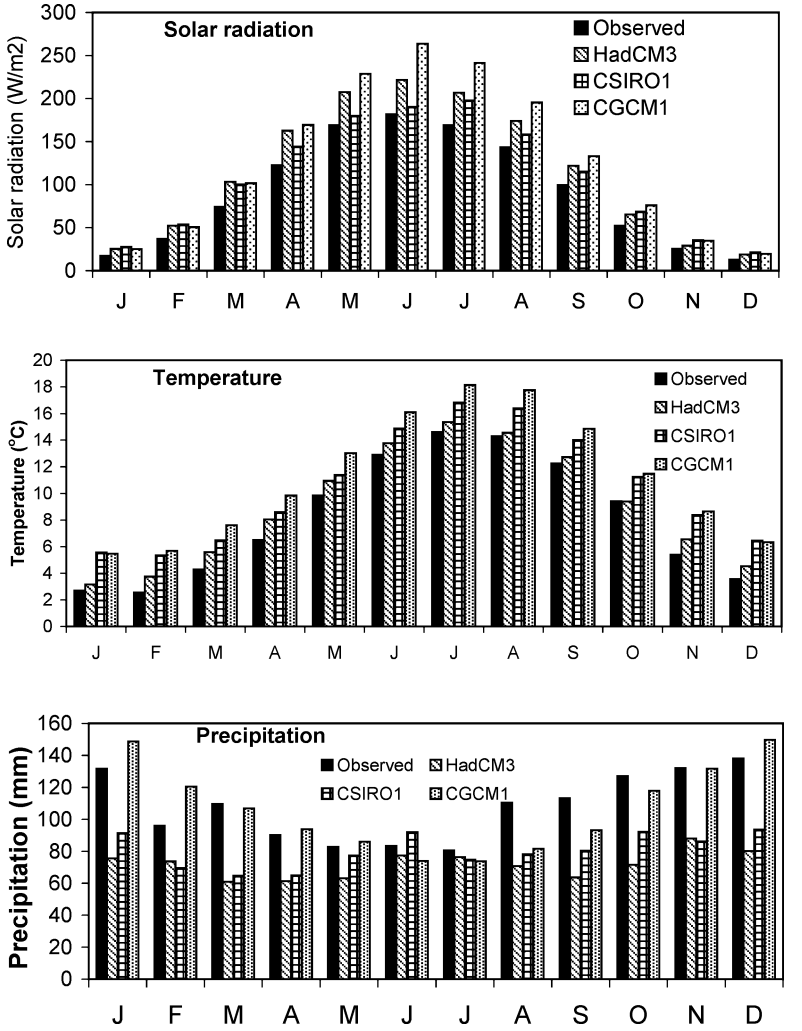

Figure 6. GCM performance over baseline (1961–1990) period. Data for all three catchments.

where,

VAR_i is the value for the variable (temperature, precipitation) at grid point i;
D_i^s is the distance from the site to the GCM grid point i;
VAR_D is the downscaled variable.

Before defining the climate change scenarios, it would be useful to compare the performance of the three GCMs over the baseline period. Observed and GCM simulated mean temperature, net incoming solar radiation and precipitation over the baseline period are shown in Figure 6 and Table IV provides the root mean squared difference (RMSD) between the observed data and GCM-simulations. According to the information in the table, CSIRO1 appears to be reproducing the

TABLE IV
RMS difference between observed and GCM-simulated climatological variables

GCM	Radiation (w/m^2)	Temperature (°C)	Precipitation (mm)
HadCM3	94	3	140
CSIRO1	59	8	112
CGCM2	153	11	50

TABLE V
Absolute changes (from baseline) in monthly mean temperature (°C)

Scenario	Jan	Feb	Mar	Apr	May	Jun	Jul	Aug	Sep	Oct	Nov	Dec
C2	0.3	0.5	0.2	0.3	0.5	0.8	1.1	0.8	0.7	0.9	0.4	0.5
C5	0.6	0.7	0.4	0.5	0.8	1.6	1.9	1.4	1.5	1.4	0.9	0.9
C8	1.4	1.1	1.0	1.1	1.5	2.1	2.6	2.7	2.6	2.3	1.5	1.5
A2	0.4	0.7	0.9	0.8	1.2	1.0	1.0	0.9	0.9	1.3	0.7	0.9
A5	0.7	0.9	1.4	1.5	1.8	1.6	1.7	1.6	1.6	1.8	1.6	1.3
A8	1.2	1.3	1.7	2.0	2.6	2.1	2.3	2.3	2.5	2.4	2.3	1.8
H2	0.7	0.8	0.7	0.7	0.7	0.9	0.9	1.2	0.9	0.9	0.6	0.2
H5	1.9	1.4	1.3	1.2	1.7	1.8	1.8	2.5	2.3	2.0	1.0	1.2
H8	2.1	1.8	1.7	2.0	2.5	2.9	2.8	3.5	3.2	2.6	1.8	1.3
	2.7	*2.6*	*4.3*	*6.5*	*9.9*	*12.9*	*14.6*	*14.3*	*12.3*	*9.4*	*5.4*	*3.6*

C: CGCM1, A: CSIRO1, H: HadCM3, 2: 2010–39, 5: 2040–69, 8: 2070–99.
Baseline temperature in italics. Changes apply to all three catchments.

observed baseline solar radiation most adequately (RMSD = 59 w/m^2). Observed temperature is being modelled well by HadCM3 (RMSD = 3°C) while CGCM1 is performing most adequately in reproducing observed precipitation (RMSD = 50 mm).

A number of factors contribute to the differences in GCM simulation of observed climate for the same region. These include differences in horizontal and vertical resolution, differences in the representation of sub-grid physical process, (e.g. cloud formation and precipitation), model numerical schemes, and feedback mechanisms. Given that sub-grid processes are reported to be the greatest source of errors in GCMs (Risbey and Stone, 1996) - perhaps even more than their inadequate resolution, then different representations of these processes are most likely responsible for the differences in GCM output. Differences in the type of model numerical scheme may also be responsible for possible differences. The two types of numerical schemes used in GCMs are grid point schemes and spectral schemes (McGuffie and Henderson-Sellers, 2001). The former represent the data on a finite grid over the globe, in both height and latitude/longitude, whilst the latter represent their variables as spherical harmonics.

TABLE VI
Absolute changes (from baseline) in monthly mean net solar radiation (w/m^2)

Scenario	Jan	Feb	Mar	Apr	May	Jun	Jul	Aug	Sep	Oct	Nov	Dec
C2	0.5	−2.3	−10.4	5.8	20.9	1.2	13.4	5.6	3.5	6.4	3.7	0.9
C5	0.4	−2.4	−10.3	1.4	21.7	5.1	−4.9	−7.6	0.1	7.5	3.6	1.6
C8	−0.2	1.3	−6.5	8.2	16.3	18.6	−13.2	−10.1	0.6	5.5	5.3	1.1
A2	1.0	−1.2	−5.0	7.8	13.6	7.7	4.6	−8.9	−6.9	1.3	1.4	−0.6
A5	1.7	3.0	−9.2	−1.2	13.5	27.2	5.7	−3.4	−4.8	−0.9	−0.3	−0.8
A8	−0.1	2.8	−11.9	5.4	−4.5	24.2	−7.3	−3.3	−6.6	2.4	−4.0	−0.6
H2	−2.5	−0.4	−7.7	−5.6	8.3	21.9	8.6	4.1	11.7	3.1	2.8	−1.3
H5	−3.9	0.8	−5.0	7.1	11.4	13.7	22.8	15.0	30.7	6.3	3.3	−2.3
H8	−2.6	−2.6	−0.1	5.8	12.1	15.8	28.9	15.3	31.0	4.1	0.3	−0.5
	51.2	*108.2*	*224.5*	*338.3*	*455.7*	*492.7*	*485.3*	*394.4*	*261.3*	*153.9*	*67.9*	*35.4*

C: CGCM1, A: CSIRO1, H: HadCM3, 2: 2010–39, 5: 2040–69, 8: 2070–99.
Baseline net solar radiation in italics. Changes apply to all three catchments.

TABLE VII
Absolute changes in monthly mean precipitation (mm)

Scenario	Jan	Feb	Mar	Apr	May	Jun	Jul	Aug	Sep	Oct	Nov	Dec
C2	−5.0	19.0	33.3	2.1	−20.5	−4.6	−14.9	−6.8	−12.3	−21.1	−7.5	5.5
C5	16.8	21.8	42.2	−2.1	−13.5	−13.9	9.1	8.0	−4.0	−29.2	2.9	10.3
C8	33.2	17.0	46.9	6.9	−8.9	−25.7	11.3	5.5	−1.4	−7.5	−6.5	7.3
A2	−2.0	27.1	28.9	3.3	7.4	7.0	9.1	18.6	16.3	−17.8	6.6	33.4
A5	−14.7	6.5	35.7	17.7	7.4	−5.2	4.8	17.4	12.1	−2.5	14.2	33.5
A8	18.0	7.3	52.7	17.5	30.2	−19.1	11.1	18.0	8.2	7.1	58.0	43.0
H2	11.5	−14.4	1.4	3.3	0.7	−30.0	−26.6	−21.6	−11.9	−7.4	8.6	16.1
H5	37.8	1.8	22.3	−8.6	−20.2	−29.8	−44.8	−59.8	−60.3	5.8	−4.8	50.3
H8	48.1	13.7	10.9	6.0	−9.4	−32.6	−53.2	−55.6	−46.7	12.9	18.6	36.3
	136.1	*98.2*	*112.7*	*93.1*	*83.8*	*85.7*	*83.7*	*113.8*	*115.4*	*130.7*	*137.9*	*146.4*

C: CGCM1, A: CSIRO1, H: HadCM3, 2: 2010–39, 5: 2040–69, 8: 2070–99.
Baseline precipitation in italics. Changes apply to all three catchments.

Scenarios representative of the climate in the 2020s (2010–39), 2050s (2040–69) and 2080s (2070–99) compared to the baseline (1961–1990) were used. The complete range of climate change scenarios expressed as absolute monthly changes in temperature, net solar radiation and precipitation from the baseline are provided in Tables V–VII.

An examination of the scenarios in Tables V–VII reveals that whilst the temperature changes appear to be uniform, there is less uniformity in the projected radiation and precipitation changes. Annual changes in temperature are more marked for the HadCM3 and CSIRO GCMs. The projected temperature changes from the HadCM3 and CSIRO GCMs for 2010–39, 2040–69 and 2070–99 are 0.8°C, 1.7°C, 2.4°C, and 0.9°C, 1.5°C, 2.0°C respectively. The CGCM1 gives only 0.6°C,

1.1°C & 1.8°C temperature rise for 2010–39, 2040–69 and 2070–99, respectively. This is because the CGCM1 experiment includes the cooling effect of sulphate aerosols. It should be noted that the estimation of the climate sensitivity of both the CGCM1 and HadCM3 (Table III) does not take into account the effects of sulphate aerosols hence the reason for the similarity.

The CSIRO GCM is indicating generally wetter conditions year-round in future, whilst the HadCM3 suggests wetter winters and drier summers. Indeed, opposite GCM projected changes in precipitation have also been reported by other investigators. For example, Doherty and Mearns (1999) found that CGCM1 and HadCM2 model simulated opposite changes in seasonal precipitation over North America. The reasons for differences between different GCMs in simulating future climate given the same CO_2 forcing (in the present case, the same forcing is used by HadCM3 and CSIRO1) are the same as those discussed earlier and may be attributable to different model parameterisations.

3.4. APPLYING THE SCENARIOS

It is usually straightforward to perturb baseline climate using a "simple perturbation" approach in which mean monthly climatic changes are applied to baseline climate. However, a limitation of such an approach is that the temporal structure (such as length of dry periods and interannual variability) of the perturbed records will be the same as the historic record. To overcome this limitation, the Long Ashton Research Station Weather Generator (LARS-WG) (Racsko et al., 1991) was used to generate climate-perturbed data series which does not suffer from this limitation. LARS-WG uses observed daily precipitation, minimum temperature, maximum temperature, and net solar radiation to simulate data. Future time-series may also be generated providing that temperature, radiation and precipitation scenarios (with respect to mean and standard deviation changes) are defined.

The simulation of precipitation occurrence is based on distributions of the lengths of continuous sequences, or series of wet and dry days. This is different to the more commonly used approaches (e.g. Richardson, 1981) which applies a first order Markov model to describe wet and dry day occurrence. The limitation of the Markov model approach is that it has "limited memory" of rare events (Semenov and Barrow, 1997) and as such, may not reproduce long dry or wet series at particular locations (Rackso et al., 1991). In LARS-WG this limitation is overcome by using the series approach, where the distribution of wet and dry series is obtained from observational records. Mixed exponential distributions are used to model both the wet and dry series and rainfall amount on a wet day. The distribution of the other climate variables; minimum and maximum temperature, and solar radiation is based on current system status (i.e. whether a wet or dry series). Wet series are defined as continuous sequences of days with rainfall equal to or greater than 0.1 mm. The lengths of wet and dry series are modelled with mixed exponential distributions.

Scenarios defined earlier were supplied to LARS-WG along with observational climate data for simulation. Net solar radiation data for Yorkshire were unavailable, and sunshine duration data were supplied to the model instead. LARS-WG uses these data to internally obtain estimates of radiation from the latitudinal short-wave radiation emitted by the Sun, R_a. The formula of Prescott (1940) is used by the model:

$$R_s = R_a(a + b\,n/N) \tag{3}$$

where,

R_s = net incoming (short-wave) solar radiation (W/m^2);
R_a = latitudinal short-wave radiation emitted by the Sun (W/m^2) – determined from meteorological tables;
n = observed number of sunshine hours; N = theoretical maximum sunshine hours at a specified location (from meteorological tables);
a = percentage of R_a reaching the Earth's surface on a completely cloud-covered day;
b = percentage of R_a absorbed by the clouds on a completely cloud-covered day.

Meteorological tables are used by the model to estimate R_a and N, and regression expressions of Rietveld (1978) defining $a = 0.10 + 0.24\,n/N$ and $b = 0.38 + 0.08\,N/n$ are used by the model. Values of n and R_a for Yorkshire are provided in Table II.

LARS-WG has been applied in impacts studies by Semenev and Porter (1994), and Semenev and Barrow (1997). Faulkner et al. (1997) compared its performance with a first and second-order Markov chain model at three UK sites. The comparison was based on the mean and standard deviation of (i) monthly rainfall, (ii) monthly maximum 1-day rainfalls and (iii) lengths of dry spells. An additional test was to compare the number of dry spells with a minimum 10-day duration. On the basis of these tests, Faulkner et al. (1997) concluded that LARS-WG was the best model overall for reproducing statistics of observed rainfall.

LARS-WG was calibrated using baseline climate data and the parameters were then perturbed. Daily GCM data were used to calculate 2010–39, 2040–69 & 2070–99 changes (from baseline) in precipitation intensity, duration of wet and dry days and temperature means and variances. These changes were then applied to LARS-WG parameters previously calculated from the observed daily data. The perturbed parameters were used to generate 30 years of daily data for the three GCMs and three time periods (2010–39, 2040–69 & 2070–99). A new sequence of daily climatic variables (temperature, radiation and precipitation) representing the future was thus produced. The average monthly precipitation simulated by LARS-WG is compared to observed data in Table VIII. As shown in the table, the relative differences between observed and simulated precipitation seldom exceeds 15% demonstrating the adequacy of LARS-WG in reproducing mean monthly runoff. The LARS-WG also reproduced other statistics of the observed data reasonably

TABLE VIII
Comparison of observed and LARS-WG simulated precipitation

	Gorple			Widdop			Walshaw Dean			Luddenden			Ogden		
	Obs	Sim	% Diff	Obs	Sim	% Diff	Obs	Sim	% Diff	Obs	Sim	% Diff	Obs	Sim	% Diff
Jan	152	160	−5.6	143	149	−4.2	140	148	−5.8	107	111	−3.5	107	107	−0.1
Feb	110	113	−2.4	102	110	−7.8	101	97	3.5	84	85	−1.1	80	77	4.2
Mar	127	130	−2.5	124	132	−6.5	120	114	5.0	96	85	11.0	91	90	1.2
Apr	97	98	−1.2	92	82	11.4	97	98	−0.5	80	99	−23.1	78	72	8.1
May	92	81	12.0	85	74	12.8	92	92	−0.3	76	74	2.7	75	72	2.8
Jun	92	102	−11.8	90	79	11.9	87	86	1.3	80	76	4.1	72	74	−2.2
Jul	91	96	−6.4	91	89	2.3	88	84	4.6	64	68	−5.8	64	62	2.2
Aug	123	124	−0.9	123	107	12.6	118	124	−5.7	93	94	−1.1	88	81	7.7
Sep	126	122	3.5	121	128	−5.7	125	135	−7.6	99	109	−10.3	94	92	2.6
Oct	143	172	−20.0	140	166	−19.1	134	139	−3.7	109	113	−4.4	109	101	6.9
Nov	155	158	−2.0	149	142	4.2	147	153	−4.0	111	111	0.3	106	105	0.7
Dec	161	161	−0.1	156	150	3.7	150	157	−4.8	111	107	3.4	114	111	3.1

All values excluding differences in mm.

well. It is acknowledged that by applying the weather generator, a further source of modelling uncertainty is introduced into the assessment, which is ignored in the current study.

3.5. POTENTIAL EVAPOTRANSPIRATION

A requirement of the MODHYDROLOG is daily potential evapotranspiration (PE). Since LARS-WG did not simulate this variable, some way had to be found to transform the LARS-WG temperature and net radiation (baseline and future simulated data) to PE. As well as simulating future PE, it was decided to simulate baseline PE also rather than using the observed PE. This is to allow modelling errors in simulated baseline and future PE to cancel each other out.

The Bowen ratio method (see Shuttleworth, 1993) was employed for the conversion. This method uses an energy-balance approach to determine the evaporation rate in mm (E) (Chow et al., 1988) as follows:

$$E = \frac{R_n - G}{(\vartheta \rho_w)(1 + b_r)} \tag{4}$$

where,

R_n = net surface solar radiation (MJ/m^2/day);
ϑ = latent heat of vapourisation of water (MJ/kg) = $2.501 \times 10^6 - 2370T$ where T is the temperature in °C.
ρ_w = water density (kg/m^3) = 1000 kg/m^3 for temperatures between 0°C and 10°C and reduces by 1 kg/m^3 for every 5°C rise in temperature;
b_r = Bowen ratio - which is the ratio of sensible heat flux and water vapour heat flux.
G = energy exchanged between the water body and the surrounding ground (MJ/m^2/day).

R_n was estimated using:

$$R_n = R_s(1 - \alpha) - \sigma T^4(0.56 - 0.09\sqrt{e_d})\left(0.1 + 0.9\frac{n}{N}\right)$$

where R_s is calculated using Equation (3), α is the albedo (=0.05), T is the air temperature (°K), σ is the Stefan-Boltzmann constant ($=4.903 \times 10^{-9}$ MJm^{-2} °K^{-4} day^{-1}), and e_d is the saturation vapour pressure at dew point temperature (kPa) and n and N are as defined previously. In the application of equation (4), G was ignored, which is reasonable if the day-to-day variation in temperature is negligible (see Shuttleworth, 1993) as assumed for the sites.

The Bowen ratio method requires, in addition to radiation and temperature data, the specific heat capacity at constant pressure and the heat diffusivity data. These data were however unavailable with which to calculate the Bowen ratio, therefore an alternative approach, utilising evaporation data at Gorple site (see Table II) was employed. This involved (i) computing evaporation based on baseline radiation

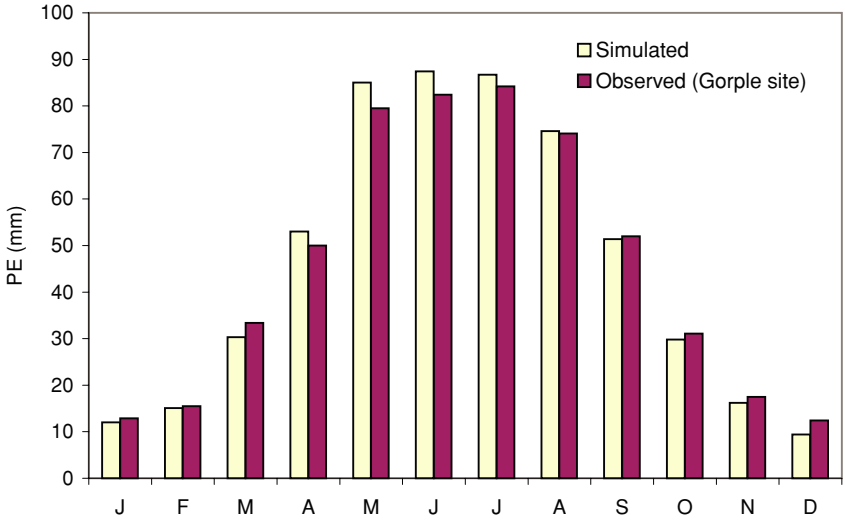

Figure 7. Comparison of monthly mean observed and simulated potential evapotranspiration.

(determined using Eqn. (4) and temperature data by setting the Bowen ratio to 1 and, (ii) varying the Bowen ratio in a trial-and-error manner in order to match the calculated evaporation with the observed Gorple evaporation. Having determined the Bowen ratio, the evapotranspiration based on LARS-WG simulated temperature and radiation could be readily factored from E as described in section 3.2, thus producing baseline and future daily potential evapotranspiration time-series data. A comparison of observed and simulated PE is provided in Figure 7. Although, PE is being slightly over-estimated during April–August and under-estimated during the remaining part of the year, there is generally good agreement between both observed and simulated PE.

4. Results and Discussion

4.1. HYDROLOGIC MODELLING

MODHYDROLOG was used for modelling the daily runoff and model calibration was carried out using daily data over 1962–1975 with validation based on daily data over the period 1976–1990. Model performance was excellent during calibration with an R^2 exceeding 0.96. Performance over validation, though not as good as that over calibration, was generally adequate with R^2 exceeding 0.87. Figure 8 compares the observed and simulated runoff at the largest sub-catchment catchment (Walshaw Dean) during calibration and validation. Both fits are very good. With regard to low flows, which is most relevant part of the hydrographs for water resources, the observed and simulated flows are in close agreement.

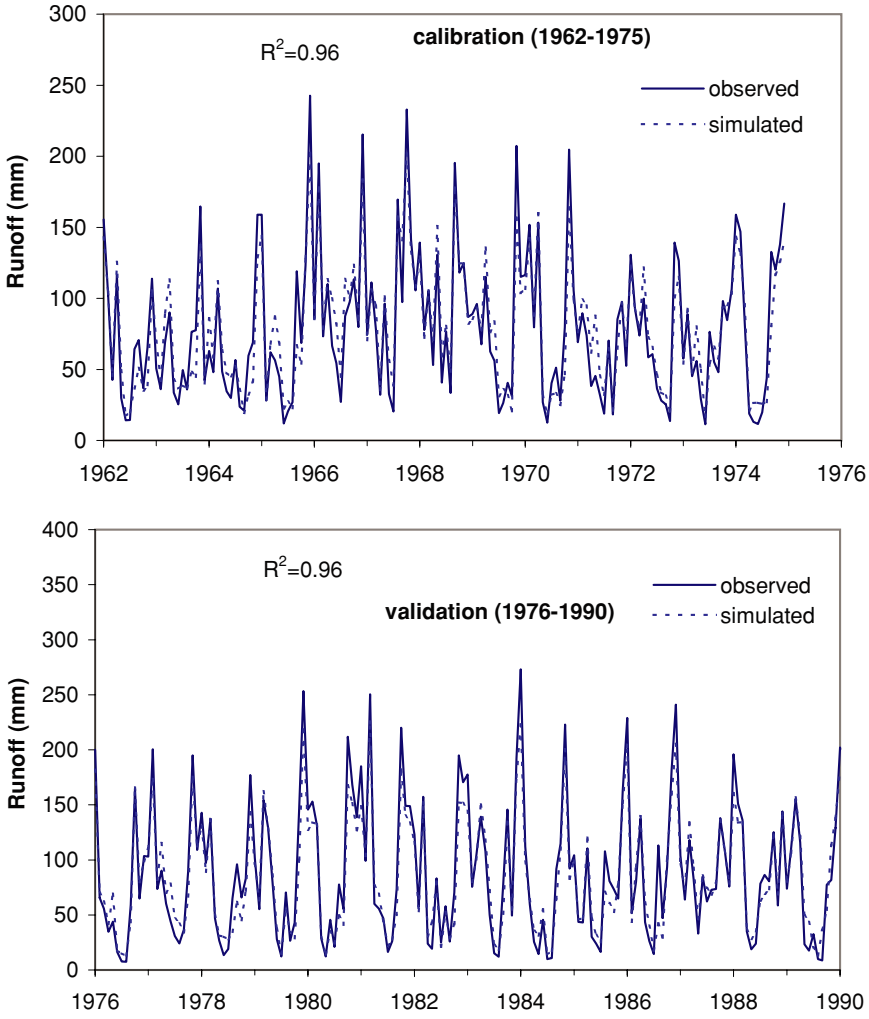

Figure 8. Hydrographs of MODHYDROLOG monthly flows at Walshaw Dean sub-catchment.

4.2. RUNOFF SENSITIVITY TO CLIMATE CHANGE

After simulating the "one off" baseline and "future" daily runoff time-series for each of the climate change scenarios, one thousand replicates of the baseline-future pair of monthly runoff were obtained using the AR(1) model along with the V-S scheme described in Section 2.3. Table IX provides a comparison of observed and generated runoff at Hebden site. The percentage differences are all below 13% indicating adequate reproduction of the mean runoff statistic. The average changes in runoff based on the 1000-paired replicates were then determined. These are presented for nine climate change scenarios in Figure 9. For lack of space, results are only presented for

TABLE IX
Comparison of observed and generated runoff at Hebden site (1961–1990)

Month	Observed runoff (mm)	Generated runoff* (mm)	Percentage difference
Jan	138	153	−11
Feb	101	112	−11
Mar	95	104	−9
Apr	72	71	2
May	44	46	−3
Jun	33	37	−12
Jul	32	34	−8
Aug	52	49	6
Sep	66	66	1
Oct	102	115	−13
Nov	124	127	−3
Dec	142	150	−6

*Based on the average of 1000 traces.

the lumped catchments which were obtained by considering all the three main catchments (Hebden, Luddenden and Ogden) as one large catchment. This is valid given that the reservoir systems are considered as parallel systems. The results indicate that changes in runoff follow a similar pattern to precipitation changes presented earlier (see Table VII). For instance, the CSIRO1 scenario predicted increases in precipitation throughout most of the year with the maximum increases expected in March and November. Similarly, the CSIRO1 scenario results in an increase in runoff during most of the year with maximum increases expected in March and November (see Figure 9).

The scenarios based on the CGCM1 and HadCM3 GCMs are showing a tendency for reduced runoff during the summer. The largest reduction in runoff results from HadCM3 in September during 2040–69 (66% = 38 mm) whilst the largest increase of 54% (59 mm) is expected under the CSIRO1 in November during 2070–99. Such large reductions will no doubt lead to significant reductions in future reservoir yield, when the storage capacity is fixed.

4.3. CLIMATE CHANGE IMPACTS ON RESERVOIR YIELD AND ITS SAMPLING UNCERTAINTY

The yield assessment involved determining 1000 yield changes (from baseline) for existing storage capacity of 11.13×10^6 m^3 (30% MAF) which is the capacity of the five-reservoir system. As noted earlier, the SPA is essentially a reservoir capacity

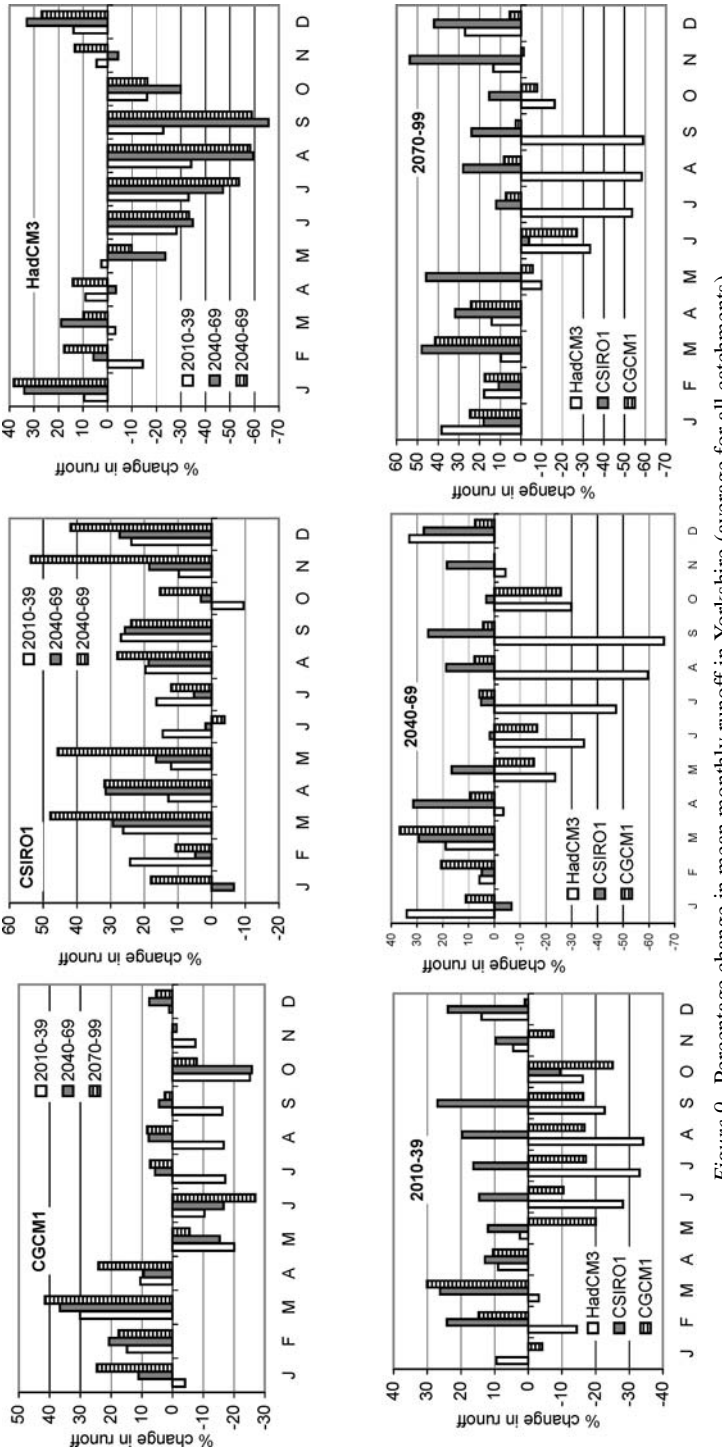

Figure 9. Percentage change in mean monthly runoff in Yorkshire (average for all catchments).

estimation tool, and yield estimates for a given storage capacity were obtained by constructing the storage-yield-reliability functions. Figure 10 shows the empirical distribution of the yield changes. The *one-off* yield change based on the traditional single records approach is also shown in the figure. What the box plots highlight is the range of likely impacts on yield, which is not captured by the use of a single historic record.

Information extracted from the figure (for 100% time-based reliability corresponding to an almost no failure risk) is presented in Table X. It can be seen from the table that based on the traditional approach, yield changes vary from −1.8% to +2.8% for the CGCM1 scenarios. However, use of the extended Monte Carlo approach enables the examination of the various possibilities of yield changes. For example, the 90th and 10th percentiles range respectively from 0.2 to 4.4 and −5.4 to −3.2 for these scenarios. The change in the median is from −2.7% to +0.7%. The mean and median results indicate a reduction in yield by 2010–39 and a subsequent increase by 2040–69 and 2070–99. This pattern of change is consistent with the runoff changes presented in Figure 9. It may be recalled that the CGCM1 scenarios resulted in summer runoff reduction by 2010–39 whilst small increases in runoff were expected throughout most of the year by 2040–69 and 2070–99.

The changes in yield resulting from the CSIRO1 scenarios are more extreme than the CGCM1 based changes. For these scenarios, results based on the traditional approach indicate that the reservoirs will be able to provide more water in the future. The increased reservoir yield is expected to amount to 10.5%, 9.5% and 10.5% by 2010–39, 2040–69 and 2070–99, respectively. However, based on the Monte Carlo approach, it is clear that the yield changes can vary widely (e.g. for 2010–39, from an increase of 1.9% (10th percentile) to an increase of 9.9% (90th percentile). As with yield changes resulting from CGCM1, the CSIRO1 yield changes can be traced back to runoff changes that were summarised in Figure 9. It can be recalled that the CSIRO1 scenarios resulted in increased runoff throughout the year in the future.

In contrast to the CSIRO1 results, yield changes resulting from the HadCM3 scenarios indicate reductions. Based on the traditional approach, the reductions range from -1.2% (2010-39), −8.2% (2040–69) and −3.7% (2070-99). However, when sampling uncertainty was considered, the changes range from a minimum of −14.3% (2040–69) to a maximum of +0.2% (2070–99).

Highlighted in Table X (in bold font) are the most severe changes in yield that can be expected to occur based on the traditional and Monte Carlo approach. Based on the traditional approach, the largest rise in yield results from the CSIRO1 2070–99 (A8) scenario (10.5%). On the other hand, the largest reduction results from HadCM3 2040–69 (H5) scenario (−8.2%). Based on the Monte Carlo results, these changes are +14.5% (A8) and −14.3% (H5). The current yield from the aggregated system is 60.9 Megalitres/day (Mld). Based on the traditional approach and according to all scenarios and to maintain the high levels of performance (almost no failure risk), future yield could vary between 55.9 Mld and 67.3 Mld. However,

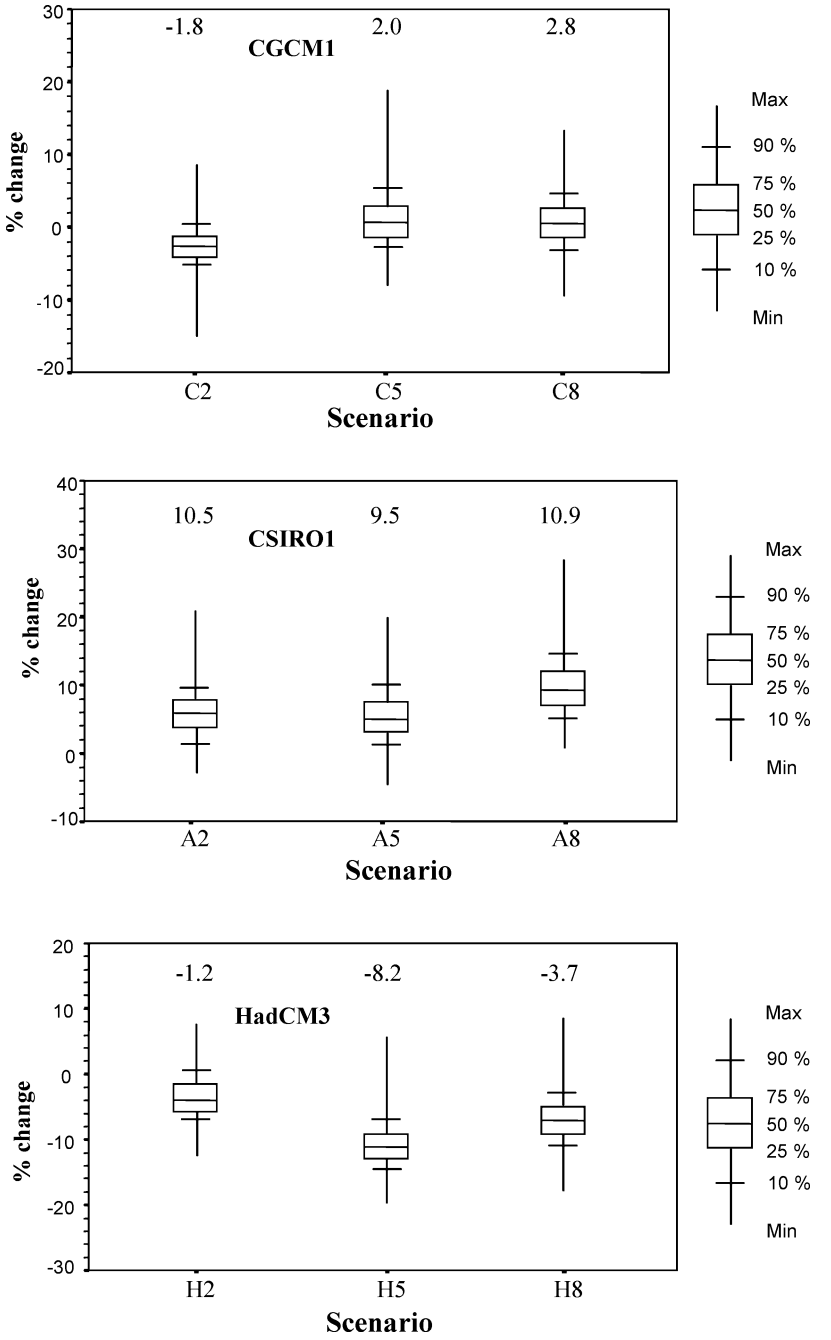

Figure 10. Box plots of yield changes for different climate scenarios (storage = 31% of MAF; C = CGCM1; A = CSIRO1; H = HadCM3; 2 = 2010–39; 5 = 2040–69, 8 = 2070–99; numbers above box-plots indicate the "one-off" yield change).

TABLE X
Percentage change in yield (from baseline) for aggregated reservoir systems resulting from climate change scenarios

Scenario	Single Record Method	Monte Carlo Method			
		Mean	Median	90th Percentile	10th Percentile
C2	−1.8	−2.6	−2.7	0.2	−5.4
C5	2.0	0.9	0.7	5.1	−2.8
C8	2.8	0.6	0.5	4.4	−3.2
A2	10.5	5.9	5.8	9.9	1.9
A5	9.5	5.5	5.3	10.0	1.3
A8	**10.5**	9.7	9.4	**14.5**	5.0
H2	−1.2	−3.7	−4.0	0.2	−7.5
H5	**−8.2**	−10.9	−11.1	−7.4	**−14.3**
H8	−3.7	−6.9	−7.1	−3.0	−10.7

Bold font indicates extreme changes in yield for the reservoir system (near 100% reliability).
C: CGCM1, A: CSIRO1, H: HadCM3, 2: 2010–39, 5: 2040–69, 8: 2070–99.

based on the Monte Carlo approach, future yield is likely to show greater variations; between 52.2 Mld and 69.7 Mld.

4.4. COMPARISONS WITH OTHER STUDIES

There have been few studies, if at all, on the variability of yield impacts to which the current results can be directly compared. This is in contrast to the vast array of studies on runoff impacts, although the majority of these studies have only looked at the mean impacts rather than the distribution of these impacts.

Arnell (1999) applied HadCM3 to some European rivers (Volga, Rhine and Danube) and found annual precipitation changes for 2040-69 to range from −12% to +1%, annual PE changes to range from 30%–37% and annual runoff varied from −20% to −35%. Although the annual runoff changes are severer than those found in this study, the reductions in future runoff are in agreement with this study.

Chiew et al. (1995) used five GCMs including previous versions of CGCM1 and CSIRO1 (i.e. uncoupled versions) GCMs to investigate the sensitivity of runoff to climate change by the 2030s. The study considered 28 unregulated catchments across Australia ranging in size from just 3 km^2 to 2500 km^2. They noted that all GCMs resulted in increased annual runoff of up to 25% by 2030 in the humid tropical catchments of north-east coast of Australia. In contrast, there was little agreement amongst the GCMs as regards to runoff impacts in other parts of Australia. For example, runoff changes of ±20% were expected in south-east Australia. Unfortunately, Chiew et al. (1995) made no distinction as to which GCM gave which

changes. The results for the south east of Australia confirm that, as found in the present study, different GCMs can lead to opposite effects on runoff.

Wolock and McCabe (1999) also noted the opposite effects on runoff of climate change scenarios from two different GCMs. They used two climate scenarios, CGCM1 and HadCM2 in an assessment of the sensitivity of US water resources to climate change. They found that the HadCM2 scenario generally resulted in increased runoff over much of USA by the 2030s with a maximum increase of 245% expected in the lower Colorado. In contrast, the CGCM1 resulted in reductions in runoff by the 2030s with an expected maximum reduction of 87% in Texas and the Gulf of Mexico.

A scenario based on CGCM1 was also adopted by Dvorak et al. (1997). However, their assessment considered the rainfall-runoff response of four temperate European catchments (in the Czech Republic) with catchment sizes ranging from 94 km^2 to 50,762 km^2. The impacts assessment revealed that the CGCM1 projected 7% increase in precipitation (plus a 3.1°C rise in temperature) resulted in changes in runoff over the four catchments ranging from -10% to $+2\%$. The opposite changes in runoff are probably due to different changes in PE resulting from the same temperature rise in the different catchments.

The studies discussed so far were all based on the traditional single record impacts assessment methodology. It is also interesting to briefly discuss some other studies that have adopted a limited Monte Carlo sampling methodology. For instance, Nikolaidas et al. (1994) showed annual runoff changes varied by $\pm 24\%$ based on a Monte Carlo approach. On the other hand, results from deterministic modelling using two climate change scenarios resulted in reductions in annual runoff of 37.5% and 17.9%, respectively.

4.5. IMPLICATIONS FOR WATER MANAGERS

Results from the present study have confirmed that mean impacts which have received so much attention from climate impacts studies could be misleading because large variability in this mean is possible, given the usual length of streamflow data records available for water resources planning and operational studies in practice. By being aware of such variability, water managers are better able to plan climate change mitigating measures. Specific impacts are viewed against their associated risks of happening and intervention measures are devised appropriately. In other words, impacts which have very low probability of occurring should concern less than those which have a higher probability.

To gain an idea of what these measures may entail, it would be useful to look at an actual drought episode in Yorkshire in 1995 and its aftermath. Evidence indicated that changing temperature and rainfall trends across Yorkshire were responsible for the severe drought. For example, Holden and Adamson (2002) reported that mean annual temperatures in the uplands of Yorkshire were significantly higher during the

1991–2000 period compared to the 1931–1979 period. Also, total rainfall between April–October 1995 in Yorkshire was the lowest for 200 years (POST, 1995).

The immediate response to the drought was to impose hose-pipe bans, issue drought orders, inform the public on saving water, and begin the transfer of water to Yorkshire from other regions. The long-term strategy aimed to identify the reasons for water-supply system failure and put into place measures to prevent a repeat. Reasons included:

- Very low rainfall
- Unprecedented peak demands
- High levels of leakage from pipes
- Over-estimation of storage reservoir yield.

Water demand and efficiency was a key issue and the public were educated through media and press on the importance of saving water. Discussion began on the possibility of installing more water meters, although this raised all sorts of issues concerning the less affluent. The benefits were clear in that demand would reduce. For example, summer peak demands had been known to fall by up to 30% (POST, 1995) if a customer was asked to pay more for higher water-usage. Water-metering also has the advantage that it allows leaking pipes to be detected more easily since there is precise record of the water-balance. There were large reductions in water leakage as a result of pipe rehabilitation carried out over a number of years. Studies were commissioned to re-assess storage reservoir yield in Yorkshire using a similar Monte Carlo approach described in this study (see Adeloye and Nawaz, 1997) and reservoir operational strategies (especially for multiple-reservoirs) were revised. Nine years on from the drought, such measures have ensured that the Yorkshire region will be more prepared if faced with similar hydroclimatological conditions of 1995.

5. Conclusions

This study has used a Monte Carlo approach to characterise the sampling uncertainty of the climate change impacts on hydrology and yields of a water resources system in Yorkshire, England. The results have shown that yield changes can be highly variable and can be much different from mean changes often addressed in traditional, deterministic impact studies. A knowledge of such variability allows more meaningful planning of mitigating measures for climate change impacts because probabilities can be ascribed to different levels of predicted yield changes, enabling resources to be targeted as appropriate.

Another evidence, albeit not new, coming out from the study is that climate change water resources impacts are highly uncertain because of differences in GCM projections. The study used three different GCM experiments but while all the three GCMs agreed on the likely change and direction of future temperature in

the same catchments, projections of precipitation changes often varied from one GCM to another. This is a major problem for water resources impacts assessment since precipitation often has a much bigger impact on runoff than evaporation. Of the climate change scenarios used in the case study, those based on the HadCM3 GCM indicate drier future conditions whilst wetter conditions are predicted by the CSIRO1 GCM for the same catchments. Consequently, use of scenarios based on different GCMs had led to opposite impacts on the yield of the same water resources system. However, rather than worry about which of these impacts are correct, the impacts should be viewed as the likely range of projections which should all be considered when making plans for accommodating climate change.

With new climate change scenarios now emerging, especially those based on regional climate models, it would be worthwhile to repeat the exercise to see to what extent new results differ from those reported here. For better comparison, it may also be useful to conduct the impacts assessment using a physically-based hydrologic model.

Acknowledgements

The authors would like to thank Mr Ian Stevens and Dr Jason Ball (Yorkshire Water Services Ltd., UK) for providing relevant data. We are also grateful to the British Atmospheric Data Centre (BADC), UK Climate Impacts Programme (UKCIP), Climate Research Unit (CRU) at the University of East Anglia, UK, Canadian Climate Centre, and the Australian Commonwealth Scientific & Industrial Research Organisation (CSIRO), for providing data. Thanks also to Prof. Tom McMahon (University of Melbourne, Australia) for supplying MODHYDROLOG, and to two anonymous reviewers for their useful feedback on the initial draft of the manuscript.

References

Adeloye, A. J. and Nawaz, N. R.: 1997, 'The reliability of storage-yield estimates for some reservoir sites in Yorkshire', Dept. Civil & Offshore Eng., Edinburgh, 66pp.

Adeloye, A. J. and Montaseri, M.: 1998, 'Adaptation of a single reservoir technique for multiple reservoir storage-yield-reliability analysis', in Zebidi, H. (ed.), *Water: a looming crisis? Proc. Int. Conf. on world water resources at the beginning of the 21st Century, UNESCO*, Paris, pp. 349–355.

Adeloye, A. J., Montaseri, M., and Garmann, C.: 2001, 'Curing the misbehaviour of reservoir capacity statistics by controlling shortfall during failures using the modified sequent algorithm', *Water Resour. Res*. **37**(1), 73–82.

Arnell, N. W.: 1999, 'The effect of climate change on hydrological regimes in Europe: a continental perspective'. *Global Environmental Change* **9**, 5–23

Boer, G. J., Flato, G. M., Reader, M. C., and Ramsden, D.: 2000, 'A transient climate change simulation with greenhouse gas and aerosol forcing: experimental design and comparison with the instrumental record for the 20th century', *Climate Dynamics* **16**, 405–425.

Cameron, D. S., Beven, K. J., Tawn, J., Blazkova, S., and Naden, P.: 2000a, 'Flood frequency estimation for a gauged upland catchment (with uncertainty)', *J. Hydrology* **219**, 169–187.

Cameron D. S., Beven, K., and Naden, P.: 2000b, 'Flood frequency estimation under climate change (with uncertainty)'. *Hydrology and Earth System Sciences* **4**(3), 393–405

Carter, T. R., Parry, M. L., Nishioka, S., and Harasawa, H.: 1994, 'Technical guidelines for assessing climate change impacts and adaptations', Intergovernmental Panel on Climate Change, University College London, Centre for Global Environmental Research, Tsukuba.

Carter, T. R., Hulme, M., and Lal, M.: 1999, *Guidelines on the use of scenario data for climate impact and adaptation assessment*, version 1, Intergovernmental Panel on Climate Change, Task Group on Scenarios for Climate Impact Assessment.

Chiew, F. H. S. and McMahon, T. A.: 1994, 'Application of the daily rainfall-runoff model MODHYDROLOG to 28 Australian catchments', *J. Hydrol.* **153**(1–4), 383–416.

Chiew, F. H. S., Whetton, P. H., McMahon, T. A., and Pittock, A. B.: 1995, 'Simulation of the impacts of climate change on runoff and soil moisture in Australian catchments', *J. Hydrol.* **167**(1–4), 121–147.

Chow, Ven Te., Maidment, D. R., and Mays, L. W.: 1988, *Applied Hydrology*, McGraw-Hill series in water resources and environmental engineering, McGraw-Hill.

Doherty and Mearns: 1999, A comparison of simulations of current climate from two coupled atmosphere-ocean GCMs against observations and evaluation of their future climates. Report to the NIGEC National Office. National Center for Atmospheric Research, Boulder, Colorado, 47 pp.

Dvorak, V., Hladny, J., and Kasparek, L.: 1997, 'Climate change, hydrology and water resources impact and adaptation for selected river basins in the Czech Republic', *Climatic Change* **36**, 93–106.

Faulkner, D. S., Arnell, N. W., and N. S. Reynard.: 1997, 'Everyday aspects of climate change in Europe', BHS 6th National Hydrology Symposium, Salford, UK.

Filliben, J. J.: 1975, The probability plot correlation coefficient test for normality, *Technometrics* **17**(1).

Flato, G. M., Boer, G. J., Lee, W. G., McFarlane, N. A., Ramsden, D., Reader, M. C., and Weaver, A. J.: 2000, 'The Canadian Centre for Climate Modelling and Analysis Global Coupled Model and its climate', *Climate Dynamics* **16**, 451–467.

Gordon, H. B. and O'Farrel, S. P.: 1997, 'Transient climate change in the CSIRO coupled model with dynamic sea ice', *Monthly Weather Review* **125**, 875–907.

Gordon, C., Cooper, C., Senior, C. A., Banks, H., Gregory, J. M., Johns, T. C., Mitchell, J. F. B., and Wood, R. A.: 2000, 'The simulation of SST, sea ice extents and ocean heat transports in a version of the Hadley Centre coupled model without flux adjustments', *Climate Dynamics* **16**, 147–168.

Hashimoto, R., Stedinger, J. R., and Loucks, D. P.: 1982, Reliability, resiliency and vulnerability criteria for water resources system performance evaluation. *Water Resources Research* **18**(1).

Hirst, A. C., O'Farrell, S. P., and Gordon, H. B.: 2000, 'Comparison of a coupled ocean-atmosphere model with and without oceanic eddy-induced advection, 1: Ocean spin-up and control integrations', *J. Climate* **13**(1) 139–163.

Holden, J. and Adamson, J., (2002), 'The Moor-House long-term upland temperature record – new evidence of recent warming', *Weather* **57**, 119–126.

Hulme, M., Mitchell, J., Ingram, W., Lowe, J., Johns, T. C., New, M., and Viner, D.: 1999, 'Climate change scenarios for global impacts studies', *Glob. Environ. Change* **9**, S3–S19.

Jones, R. G., Noguer, M., Hassell, D. C., Hudson, D, Wilson, S. S., Jenkins, G. J., and Mitchell, J. F. B.: 2004, 'Generating high resolution climate change scenarios using PRECIS', Met Office Hadley Centre, Exeter, UK, 40 pp.

Lele, S. M.: 1987, 'Improved algorithms for reservoir capacity calculation incorporating storage-dependent losses and reliability norm', *Water Resour. Res.* **23**(10), 1819–1823.

Loucks, D. P., Stedinger, J. R., and Haith, D. A.: 1981, *Water resource systems planning and analysis*, Prentice-Hall, Englewood Cliffs, N.J.

MAFF (Ministry of Agriculture, Fisheries and Food): 1967, *Potential transpiration*, Tech. Bull. 16., HMSO.

McGuffie, K. and Henderson-Sellers, A.: 2001, 'Forty Years of Numerical Climate Modelling', *Int. J. Climatol.* **21**, 1067–1109.

McMahon, T. A. and Adeloye, A. J.: 2005, *Water Resources Yield*, Water Resources Publications, Littleton, Colorado, 234 pp.

Mimikou, M. A., Baltas, E., Varanou, E., and Pantazis, K.: 2000, 'Regional impacts of climate change on water resources quantity and quality indicators', *J. Hydrology* **234**, 95–109.

Mott MacDonald: 1995, *Calder area reservoir hydrological records*, report prepared for Yorkshire Water Services Ltd., UK, ref. 28918BA01/1/B.

Nawaz, N. R. and Adeloye, A. J.: 1999, 'Evaluation of monthly runoff estimated by a rainfall-runoff regression model reservoir yield assessment', *Hydrological Sci. J.* **44**(1), 113–134.

Nikolaidis, N. P., Hu, H.-L., Ecsedy, C., and Lin, J. D.: 1993, 'Hydrologic response of freshwater watersheds to climatic variability: model development', *Water Resour. Res.* **29**(10), 3317–3328.

Nikolaidis, N. P., Hu, H-L., and Ecsedy, C.: 1994, 'Effects of climatic variability on the hydrologic response of a freshwater watershed', *Aquatic Sciences* **56**(2), 161–178.

Penman, H. L.: 1950, 'Evaporation over the British Isles', *Quart. J. Roy. Met. Soc.* LXXVI **330**, 372–383.

Pitman, A. J. and Chiew, F. H. S.: 1996, 'Testing a GCM land surface scheme against catchment-scale runoff data', *Climate Dynamics* **12**(10), 685–699.

POST – The UK Parliamentary Office of Science and Technology.: 1995, 'The 1995 Drought', Technical Report 71.

Prescott, J. A.: 1940, 'Evaporation from a water surface in relation to solar radiation', *Trans. R. Soc. S. Austr.* **64**, 114–118.

Prudhomme, C., Dörte Jakoba, D., and Svensson, C.: 2003, Uncertainty and climate change impact on the flood regime of small UK catchments, Journal of Hydrology **277**, 1–23.

Racsko, P., Szeidl, L., and Semenov, M.: 1991, 'A serial approach to local stochastic weather models', *Ecol. Modelling* **57**, 27–41.

Reungoat, A.: 2000, *Rainfall-runoff modelling with MODHYDROLOG*, unpublished MSc Thesis, Heriot-Watt University, Edinburgh, UK.

Richardson, C. W.: 1981, 'Stochastic simulation of daily precipitation, temperature and solar radiation', *Water Resour. Res.* **17**, 182–190.

Risbey, J. S. and Stone P. H.: 1996, 'A case study of the adequacy of GCM simulations for input to regional climate change assessments', *J. Climate* **9**(7), 1441–1467.

Rietveld, M. R.: 1978, 'A new method for estimating the regression coefficients in the formula relating solar radiation to sunshine', *Agricultural Meteorology* **19**, 243–252.

Sankarasubramanian, A., Vogel, R. M., and Limbrunner, J. F.: 2001, 'Climate elasticity of streamflow in the United States', *Water Resour. Res.* **37**(6), 1771–1781.

Semenov, M. A. and Barrow, E. M.: 1997, 'Use of a stochastic weather generator in the development of climate change scenarios', *Climatic Change* **35**(4), 397–414.

Semenov, M. A. and Porter, J. R.: 1994, 'The implications and importance of non-linear responses in modelling of growth and development of wheat', in Grasman, J. and van Straten, G. (eds.), *Predictability and non-linear modelling in natural sciences and economics,* Wageningen.

Shaw, E. M.: 1994, *Hydrology in Practice*, Chapman and Hall, London.

Shackley, S., Young, P., Parkinson, S., and Wynne, B.: 1998, 'Uncertainty, complexity and concepts of good science in climate modelling: are GCM's the best tools?', *Climatic Change* **38**, 159–205.

Shuttleworth, W. J.: 1993, 'Evaporation', in Maidment, D. R. (ed.), *Handbook of hydrology,* chapter 4, McGraw Hill Inc.

Smith, T. M., Leemans, R., and Shugart, H. H.: 1992, 'Sensitivity of terrestrial carbon storage to CO_2-induced climate change: comparisons of four scenarios based on general circulation models', *Climatic Change* **21**, 367–384.

Smith, J. B. and Hulme, M.: 1998, 'Climate change scenarios', in Feenstra (ed.), *Handbook on methods for climate change impact assessment and adaptation strategies*.

Thomas, H. A. and Burden R. P.: 1963, *Operations research in water quality management*, Harvard University Press, Cambridge, Mass.

Wilby, R. L. and Wigley, T. M. L.: 1997, Downscaling general circulation model output: a review of methods and limitations, *Progress in Physical Geography* **21**(4), 530–548.

Valencia, D. and Schaake, J. C.: 1973, 'Disaggregation processes in stochastic hydrology', *Water Resour. Res.* **9**(3), 580–585.

Von Storch, H., Zorita, E., and Cubasch, U.: 1993, 'Downscaling of global climate change estimates to regional scales: an application to Iberian rainfall in wintertime', *J. Climate* **6**(6), 1161–1171.

Wolock, D. M. and McCabe, G. J.: 1999, 'Estimates of runoff using water-balance and atmospheric general circulation models', *J. Amer. Water Resour. Assoc* **35**, 1341–1350.

Wood, A. W., Lettenmaier, D. P., and Palmer, R. N. (1997) Assessing climate change implications for water reservoirs planning, *Climatic Change* **37**, 203–228.

Yorkshire Water RRDY: 1991, *Re-assessment of resource design yield (RRDY) project 3: Calder area*, technical report, 1, prepared by W. S. Atkins Ltd, England.

(Received 29 December 2003; in revised form 7 December 2005)